

## Structural Reorganization of the Copper Binding Site Involving Thr<sup>15</sup> of Mavicyanin from *Cucurbita pepo medullosa* (Zucchini) upon Reduction

Yong Xie<sup>1</sup>, Tsuyoshi Inoue<sup>1,2</sup>, Yoichi Miyamoto<sup>1</sup>, Hiroyoshi Matsumura<sup>1</sup>, Kunishige Kataoka<sup>3,\*</sup>, Kazuya Yamaguchi<sup>3</sup>, Masaki Nojini<sup>3</sup>, Shinnichiro Suzuki<sup>3</sup> and Yasushi Kai<sup>1,†</sup>

<sup>1</sup>Department of Materials Chemistry, Graduate School of Engineering, Osaka University, 2-1 Yamada-oka, Suita, Osaka 565-0871; <sup>2</sup>Structure and Function of Biomolecules Group, PRESTO, Japan Science and Technology Agency, 4-1-8 Honcho, Kawaguchi, Saitama 332-0012; and <sup>3</sup>Department of Chemistry, Graduate School of Science, Osaka University, 1-14 Machikaneyama, Toyonaka, Osaka 560-0043

Received November 4, 2004; accepted November 22, 2004

Mavicyanin, a glycosylated protein isolated from *Cucurbita pepo medullosa* (zucchini), is a member of the phytoeyanin subfamily containing one polypeptide chain of 109 amino residues and an unusual type-I Cu site in which the copper ligands are His<sup>45</sup>, Cys<sup>86</sup>, His<sup>91</sup>, and Gln<sup>96</sup>. The crystal structures of oxidized and reduced mavicyanin were determined at 1.6 and 1.9 Å resolution, respectively. Mavicyanin has a core structure of seven polypeptide β-strands arranged as a β-sandwich organized into two β-sheets, and the structure considerably resembles that of stellacyanin from cucumber (CST) or cucumber basic protein (CBP). A flexible region was not observed on superimposition of the oxidized and reduced mavicyanin structures. However, the Cu<sup>II</sup>-ε-O-Gln<sup>96</sup> bond length was extended by 0.47 Å, and the Thr<sup>15</sup> residue was rotated by 60.0 degrees and O-γ1-Thr<sup>15</sup> moved from a distance of 4.78 to 2.58 Å from the ligand Gln<sup>96</sup> forming a new hydrogen bond between O-γ1-Thr<sup>15</sup> and ε-O-Gln<sup>96</sup> upon reduction. The reorganization of copper coordination geometry of mavicyanin upon reduction arouses reduction potential decreased above pH 8 [Battistuzzi *et al.* (2001) *J. Inorg. Biochem.* 83, 223–227]. The rotation of Thr<sup>15</sup> and the hydrogen bonding with the ligand Gln<sup>96</sup> may constitute structural evidence of the decrease in the reduction potential at high pH.

**Key words:** crystal structure, mavicyanin, oxidized, phytoeyanin, reduced, reduction potential.

Cupredoxins are copper proteins containing a type-I Cu<sup>II</sup> center and a polypeptide chain of 100–140 amino acids, and are known as electron transfer proteins accepting or donating a single electron to their redox partners. These proteins found in plants and bacteria are characterized by an intense electronic absorption band near 600 nm and unusual small hyperfine coupling constants in their EPR spectra (1–3). On the basis of sequence similarity, cupredoxins are categorized into four subfamilies: (i) plastocyanin-related proteins, comprising plastocyanin, amicyanin and pseudoazurin, (ii) azurins, (iii) soluble Cu<sub>A</sub> domains derived from cytochrome *c* oxidases, and (iv) phytoeyanins (4). Phytoeyanins isolated from non-photosynthetic tissues of plants exhibit a remarkably high degree of sequence identity with each other, and are distinctly different from members of the other cupredoxin groups. Based on spectroscopic properties, the glycosylation state, the domain organization of their precursors, the domain organization of the mature proteins, and copper-binding amino acids, phytoeyanins are classified into four groups: stellacyanin, plantacyanin, uclacyanin and

early nodulin groups. Except for in the plantacyanin group, which comprises spinach basic protein (SBP), cucumber basic protein (CBP), and putative blue copper protein in pea pods (PBP), type-I Cu(II) has a normal blue copper coordinated by two His, one Met and one Cys. In other phytoeyanin subfamilies, the ligands of the type-I Cu sites are two His, one Met and one Gln (5).

Mavicyanin, a glycosylated protein isolated from *Cucurbita pepo medullosa* (zucchini) peelings, contains a type-I copper ion and a polypeptide chain of 109 amino acid residues. This protein exhibits an intense absorption band in the visible region ( $\lambda_{\max} = 599$  nm;  $\epsilon = 5000$  M<sup>-1</sup> cm<sup>-1</sup>/Cu), giving it a characteristic blue color, like other cupredoxins (6). Comparison of the mavicyanin amino acid sequence, consisting of 108 amino acids lacking the first amino residue (methionine), with those of other cupredoxins showed that three copper ligands, two His and one Cys residues, are conserved, while a fourth ligand is probably the amido oxygen atom of the Gln residue. The sequence exhibits 50.5% identity with that of cucumber stellacyanin (CST) and 45.8% with that of CBP (7). The domain architecture of mavicyanin indeed reveals that it is a member of the stellacyanin group of phytoeyanins (5). The electronic absorption, circular dichroism (CD), magnetic circular dichroism (MCD), resonance Raman (RR), and EPR spectra of mavicyanin are appreciably similar to those of stellacyanin (8). The spec-

\*Present address: Department of Chemistry, Faculty of Science, Kanazawa University, Kakuma-machi, Kanazawa 920-1192.

†To whom correspondence should be addressed. Tel: +81-6-6879-7408, Fax: +81-6-6879-7409, E-mail: kai@chem.eng.osaka-u.ac.jp

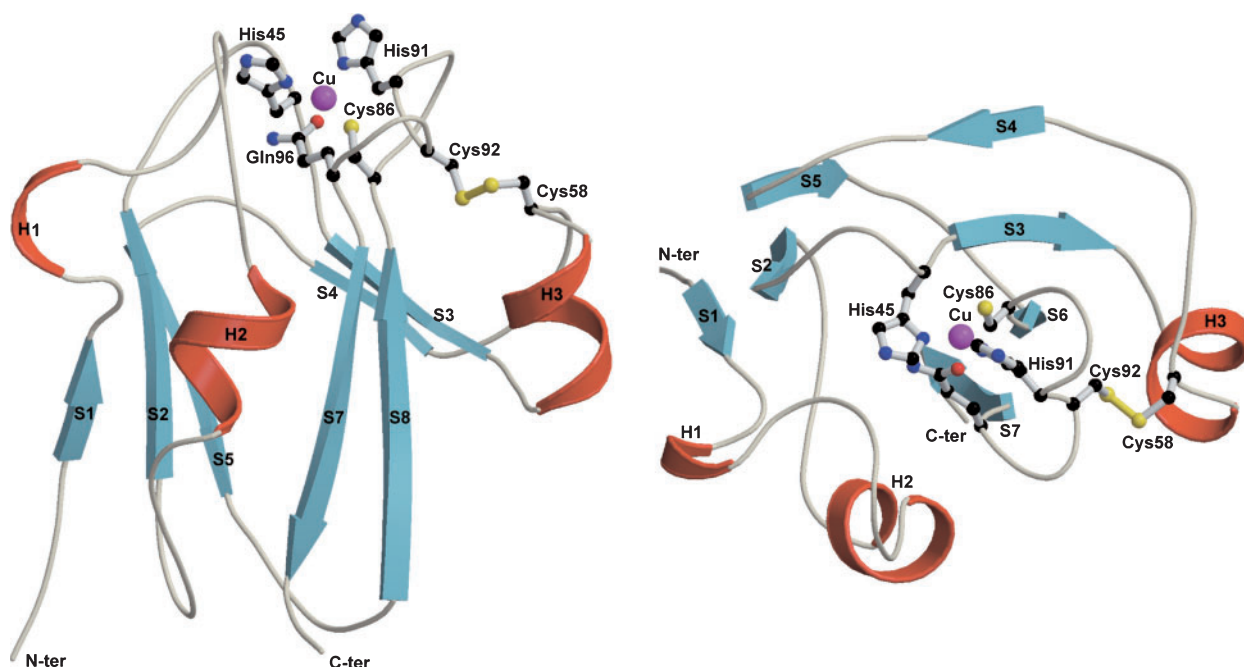


Fig. 1. Ribbon presentation of oxidized mavecyanin from *Cucurbita pepo medullosa* (zucchini) viewed from the side of the molecule (left) and from above the copper binding site (right). The  $\text{Cu}^{\text{II}}$  ion is shown as a sphere in magenta at the top of the model. Four ligands, His<sup>45</sup>, Cys<sup>86</sup>, His<sup>91</sup>, and Gln<sup>96</sup>, of the  $\text{Cu}^{\text{II}}$  ion

are represented by a ball-and-stick model. The carbon atoms, nitrogen atoms, oxygen atoms, and sulfate atoms are shown in black, blue, red, and yellow, respectively. The disulfate bond near the copper site is shown as a ball-and-stick model in yellow. All of the figures are drawn with the *MOLSCRIPT* program (26).

tropic properties of a mutant form of mavecyanin, the putative Gln ligand being replaced by Met, showed that the replacement changed the rhombic EPR signal into an axial one, and the mutant exhibited absorption and CD spectra quite similar to those of plastocyanin (9). On the other hand, a mutant form of pseudoazurin from *Achromobacter cycloclastes*, the Met ligand being replaced by Gln, showed electronic absorption and CD spectra very similar to those of mavecyanin and stellacyanin (10). These findings show that the copper ligands of mavecyanin are His, Cys, His, and an axial ligand of Gln, like in the case of stellacyanin. The roles of none of phytyocyanins have been elucidated yet.

High-resolution crystal structures of CBP (11) and CST (12) were determined in 1996. The overall crystal structures are very similar to each other. Both proteins have an overall Greek key  $\beta$ -barrel structure, which is organized into two  $\beta$ -sheets. Their copper binding sites are entirely exposed to the solvent with their copper-distal imidazole nitrogens oriented toward the surface of their molecules, in contrast to in the case of azurin, plastocyanin, and pseudoazurin. The pH-induced change in the reduction potential of CBP was examined through direct electrochemistry, it being shown that the  $E^{\circ}$  increase in the low pH region (13), like in the case of SBP (14), was caused by protonation and the detachment of a His ligand from  $\text{Cu}^{\text{I}}$  in the reduced protein. However, the pH-induced change in the reduction potential of stellacyanin from *Rhus vernicifera* showed that  $E^{\circ}$  was increased at low pH and was decreased at high pH (Sola *et al.*, unpublished results). Mavecyanin also showed an increased  $E^{\circ}$  below pH 4, and a decreased one above pH 8, like in the case of stellacyanin (15). The increasing in

$E^{\circ}$  shown by stellacyanin and mavecyanin in the low pH region should be caused by protonation and detachment of a His ligand from  $\text{Cu}^{\text{I}}$  in the reduced protein, as for CBP and SBP. Electronic spectra and NMR spectroscopy data demonstrated that the conformational change of a flexible region involving the copper binding site was expected to be cause of the  $E^{\circ}$  decrease at high pH (16). Given that the pH-induced changes in the spectral features of mavecyanin are very similar to those for stellacyanin, it is suggested that the copper coordination geometry of mavecyanin is recognized at high pH. The  $E^{\circ}$  data at high pH for mavecyanin add further elements that help characterize this transition. There is no evidence demonstrating that mavecyanin has a flexible region at high pH.

To elucidate the structural change in the copper coordination geometry upon reduction, we performed crystallographic studies on oxidized and reduced mavecyanin using a recombinant protein, a non-glycosylated form containing all of the amino acid residues of mavecyanin from zucchini and with the same spectroscopic properties (9). In this study, the crystal structures of the oxidized and reduced recombinant mavecyanin were solved at 1.6 and 1.9 Å resolution, respectively. Comparison of the two structures revealed significant changes around the copper binding site, providing structural evidence for the  $E^{\circ}$  decrease at high pH.

Crystals of the oxidized mavecyanin were obtained as described previously, and prior to data collection, the crystals were soaked in a cryoprotectant solution as reported (17). MAD data collection was performed with synchrotron radiation on beamline 40B2 of the SUPER PHOTO RING 8 (SPRING-8). The wavelengths for copper

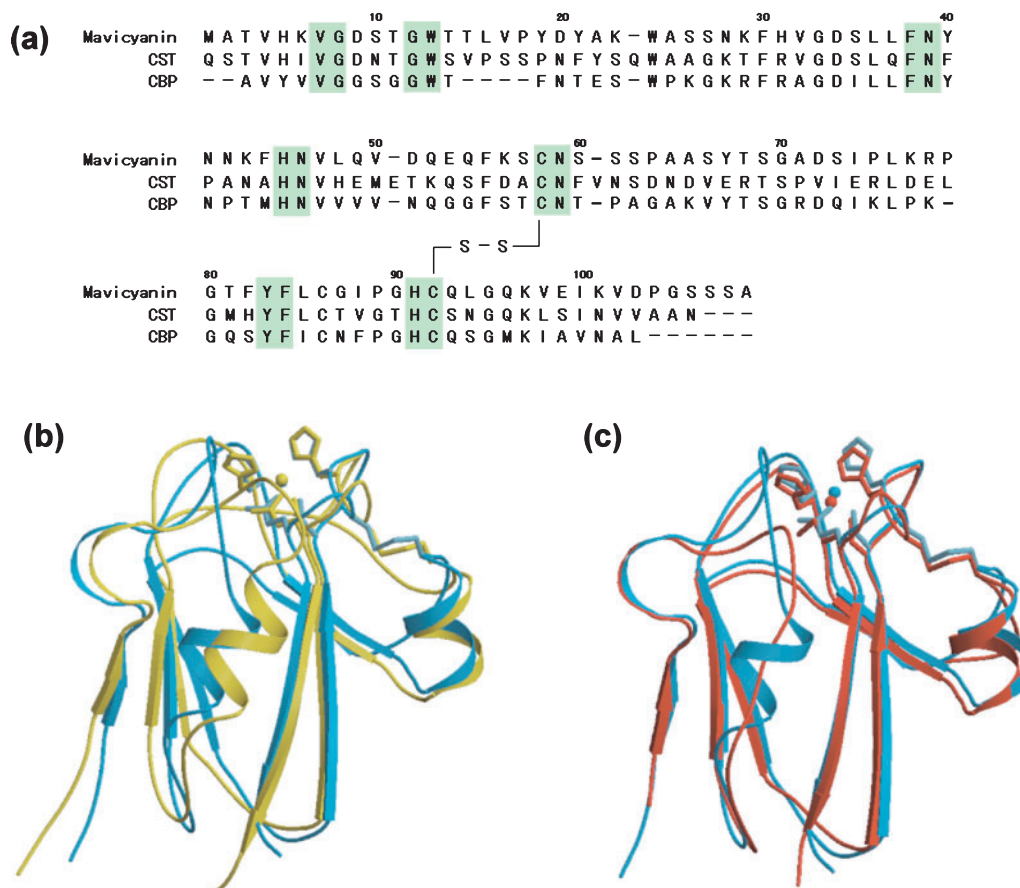


Fig. 2. Comparison of primary and crystal structures among mavicyanin, CST stellacyanin, and CBP. Sequence alignment of the amino acid sequences of mavicyanin, CST, and CBP is showed using program *ALSCRIPT* (29). The residue numbers refer to mavicyanin. Residues enclosed in green are invariant among the three

atom MAD data collection were selected based upon a fluorescence scan of a mavicyanin crystal corresponding to the K-absorption edge of the copper atom. A four-wavelengths MAD data set was collected for one mavicyanin crystal at four wavelengths: 1.305 (remote), 1.379 (peak) 1.380 (edge), and 1.393 (remote) Å at 100 K. The diffraction images were recorded using a Quantum 4 CCD detector (ADSC, USA). X-ray diffraction data were indexed, scaled, and merged using *DENZO/SCALEPACK* (18) software. MAD data were collected up to 2.0 Å resolution.

Determination of the oxidized mavicyanin structure was performed using programs in the *Crystallography and NMR System* (*CNS*; 19). Four copper positions in one asymmetric unit were identified and the subsequent MAD phase determination was performed using reflections in the 15–2.0 Å resolution range. Phase calculations were performed using *CNS* (19); giving a figure of merit calculated of 0.565, while the value was improved to 0.713 by density modification and *NCS*-averaging. Initial electron density maps in the space groups of  $P6_1$  and  $P6_5$  of an asymmetric unit were calculated at 2.0 Å resolution. The  $\beta$ -strand region of the corresponding mavicyanin molecule was observed in the electron density map calculated in the  $P6_1$  space group. Model building was

performed using the *O* (20) and *TURBO-FRODO* (21) programs. Refinement of the oxidized form structure was performed using the previously reported 1.6 Å resolution X-ray diffraction data set (17). Multiple cycles of refinement for the four independent molecules in one asymmetric unit were performed using *CNS* (19). Water molecules were added in three steps using the *WATPEAK* program in the *CCP4* program suite (23). After rebuilding the model and with several cycles of refinement, the *R*-factor and free *R*-factor were calculated to be 19.2% and 21.1%, respectively.

Like other cupredoxins, mavicyanin is readily reduced by L-(+)-ascorbic acid (5). Crystals of reduced mavicyanin were prepared by a soaking method. Oxidized mavicyanin crystals were soaked in the mother-liquid containing 10 mM sodium L-(+)-ascorbate at 293 K. The characteristic blue color of mavicyanin disappeared completely within 30 min. X-ray diffraction data were collected using a colorless crystal. Prior to data collection, the crystal was soaked in a cryo-protectant solution (17) containing 10 mM sodium L-(+)-ascorbate, and 20% (*v/v*) glycerol. X-ray diffraction data collection from the crystal of the reduced mavicyanin was performed on a Rigaku RAXIS-IV image plate using  $\text{CuK}_\alpha$  radiation from a rotating anode X-ray generator (Rigaku RU-300) with a fine-

Table 1. Comparison of the copper binding site geometry in oxidized zucchini mavidcyanin (ZMA), reduced ZMA, cucumber stellacyanin (CST), and cucumber basic protein (CBP).

	Mavidcyanin		CST	AZM121Q		CBP
	Oxidized	Reduced		Form I	Form II	
Type-I Cu (II) ligand bond lengths (Å)						
Cu–N (His1)	2.08	2.12	1.96	1.91	1.96	1.93
Cu–S (Cys)	2.17	2.22	2.18	2.13	2.11	2.16
Cu–N (His2)	1.99	2.07	2.04	2.06	2.03	1.95
Cu–O/S (Gln/Met)**	2.08	2.53	2.21	2.25	2.28	2.61
Ligand–Cu (II) ligand bond angles (deg)						
N(His1)*–Cu–S(Cys)	135	137	134	141	133	138
N(His1)–Cu–N(His2)	98	101	101	97	105	99
N(His1)–Cu–O(S) (Gln/Met)	98	90	94	87	91	83
S(Cys)–Cu–N(His2)	115	116	118	116	117	110
S(Cys)–Cu–O(S) (Gln/Met)	100	104	101	106	103	111
N(His2)–Cu–O(S) (Gln/Met)	103	97	102	98	97	112

\*His1 and His2 refer to the up- and downstream histidine ligands, respectively. \*\*In the case of CBP, the ligand is Met.

focused beam and  $\beta$ -filtered (50 kV, 100 mA) at 100 K. Diffraction data were processed and scaled using the *DENZO/SCALEPACK* (18) software. The crystal of the reduced mavidcyanin belonged to a hexagonal system of the  $P6_1$  space group, with unit-cell parameters of  $a = b = 62.7$ , and  $c = 245.9$  (Å), including 4 molecules in one asymmetric unit with a  $V_m$  value of 3.0, giving an estimated solvent content of 59%.

The crystal structure of reduced mavidcyanin was solved by a molecular replacement method using the structure of the oxidized form of mavidcyanin as a starting model with the *AmoRe* program (22) in the *CCP4* program suite (23). Refinement of the reduced mavidcyanin structure was performed using *CNS* (19). The position of the copper ion was locked at  $> 8\sigma$  peak in a  $F_o - F_c$  difference electron density map. Water molecules were added in three steps using the *WATPEAK* program in the *CCP4* program suite (23). After rebuilding the model and with several cycles of refinement, the *R*-factor and free *R*-factor were calculated to be 19.1% and 23.2% at 1.9 Å, respectively.

The crystal structure of oxidized mavidcyanin was refined at 1.6 Å resolution, and was found to consist of amino acid residues 1–104, a single copper atom and 3,569 protein atoms. All atoms are present in the final structure with the exception of the C-terminal chain from 105 to 109, because its electron density was not observed. There are 4 mavidcyanin, 329 water and 4 glycerol molecules in one asymmetric unit. The mavidcyanin molecules are related by two non-crystallographic twofold axes. The refined crystal structure of the reduced mavidcyanin model consisting of amino acid residues 1–107, 3726 protein atoms, a single copper atom, 428 water molecules and 4 glycerol molecules was observed in one asymmetric unit. All atoms are present in the final structure with the exception of Ser<sup>108</sup> and Ala<sup>109</sup>, because their electron density was not observed. Ramachandran plots generated with the *PROCHECK* program (24) showed that the two models exhibit good geometries with all residues in the most favored and additionally allowed regions.

The overall structure of mavidcyanin has a core of seven polypeptide strands arranged as a  $\beta$ -sandwich comprising two  $\beta$ -sheets,  $\beta$ -sheet I and  $\beta$ -sheet II.  $\beta$ -sheet I con-

sists of three  $\beta$ -strands: S1, residues 4–6; S2, 35–39; and S5, 71–75; and  $\beta$ -sheet II consists of four  $\beta$ -strands: S3, residues 47–50; S4, 65–67; S6, 80–85; and S7, 97–102. There are three  $\alpha$ -helices at residues 9–11 (H1), 21–26 (H2), and 52 to 57 (H3) in the loop region. H1 and H2 join S1 and S2, and H3 joins S3 and S4, respectively. At the type-I Cu site, the copper ion is coordinated by four ligands, His<sup>45</sup>, Cys<sup>86</sup>, His<sup>91</sup>, and Gln<sup>96</sup>. One disulfide bond is formed between residues Cys<sup>58</sup> and Cys<sup>92</sup> near the type-I Cu site. In Figure 1, the crystal structure of mavidcyanin is presented as a ribbon drawing.

The sequence of mavidcyanin exhibits 50.5% identity with that of CST and 45.8% with that of CBP (7). An amino acid sequence comparison among mavidcyanin, CST, and CBP is shown in Fig. 2a. Superpositioning of mavidcyanin and CST (Fig. 2b), and mavidcyanin and CBP (Fig. 2c) was performed using the *MIDAS* program (27, 28). The r.m.s. deviation of  $C_\alpha$  carbon atoms between mavidcyanin and CBP was calculated to be 0.14 Å, which is approximately equal to that between mavidcyanin and CST (0.15 Å). These results show that the overall structures of mavidcyanin, CST and CBP resemble each other considerably. Mavidcyanin should exhibit some common structural features of phytoeyanin proteins: (i) These proteins have an overall Greek key  $\beta$ -barrel structure, which is organized into two  $\beta$ -sheets. (ii) Both His ligands are entirely exposed to the solvent with their copper-distal imidazole nitrogens oriented toward the surface of the protein molecules. (iii) The Cys<sup>92</sup> residue following the His<sup>91</sup> ligand forms a disulfide bond with Cys<sup>58</sup> at the end of H3. Sequence alignment of mavidcyanin, CST and CBP showed that the two Cys residues were conserved. The crystal structures of CBP and CST include a disulfide bond formed between Cys residues like that in mavidcyanin (Fig. 2, b and c). This disulfide bond maybe play a crucial role in maintaining the tertiary structure of the protein and/or in the formation of the copper binding site because one of the His ligands of the copper binding center is followed directly by a bonding cysteine.

Superimpositioning of the oxidized and reduced structures of mavidcyanin was performed using the *MIDAS* program (27, 28). The averaged r.m.s deviation of  $C_\alpha$  carbon atoms between the oxidized and reduced structures

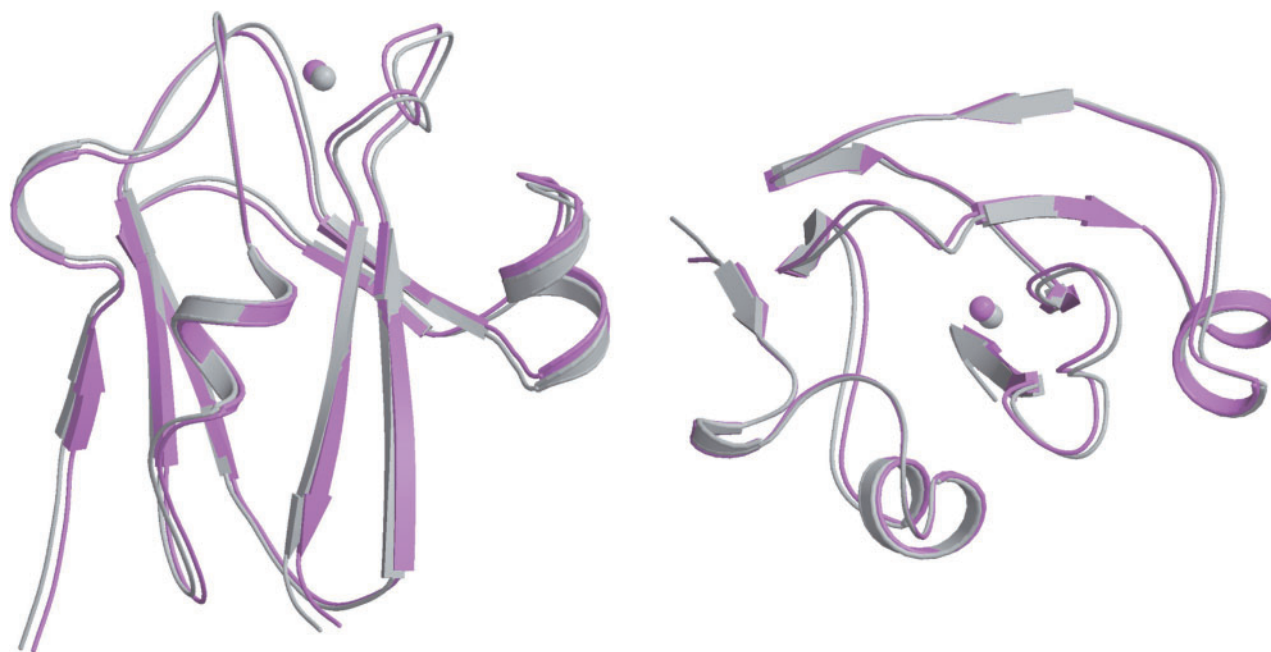


Fig. 3. Superimposition of the oxidized and reduced mavicyanin structures viewed from the side of the molecule (left) and from above the copper binding site (right). The oxidized

and reduced mavicyanin are presented as ribbon models, and are shown in grey and magenta, respectively. The  $\text{Cu}^{\text{II}}$  and  $\text{Cu}^{\text{I}}$  ions are shown as spheres, and shown in grey and magenta, respectively.

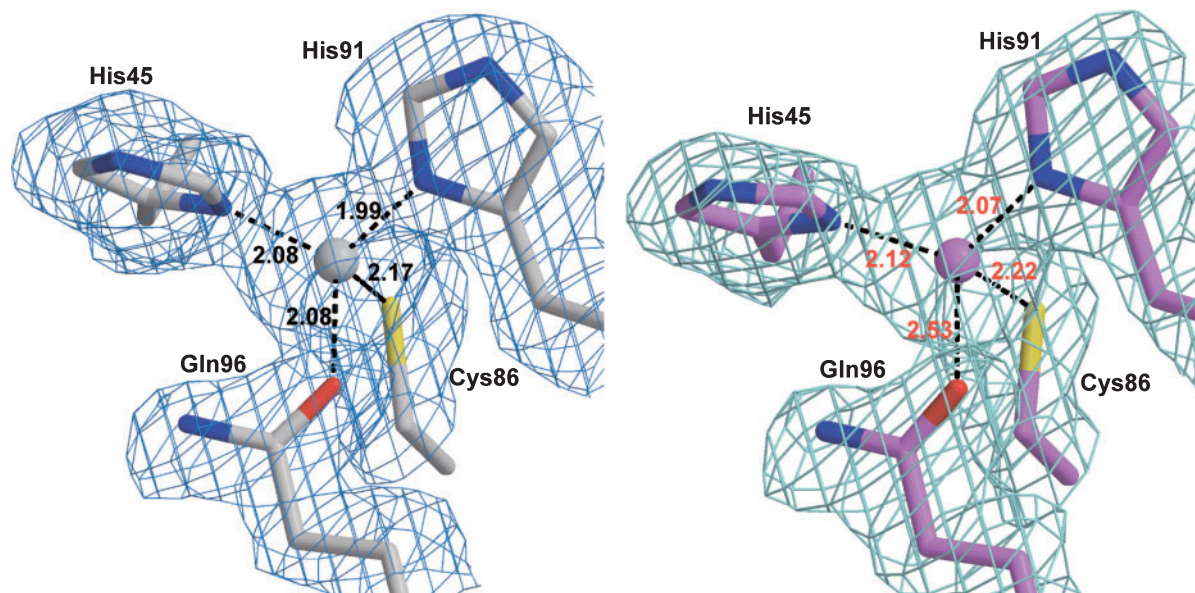


Fig. 4. Maps of the copper binding structures of oxidized (left) and reduced (right) mavicyanin, with electron density with the coefficient of  $2F_o - F_c$  omitted, calculated at 1.6 and 1.9 Å,

respectively. The distances (Å) between the ligands and the copper ion in the oxidized and reduced mavicyanin are shown in black and red, respectively.

of mavicyanin is 0.09 Å. The complete mavicyanin structure including a flexible region did not change upon reduction (Fig. 3), different from in the case of stellacyanin (16).

In the copper binding site of oxidized mavicyanin, the  $\text{Cu}^{\text{II}}$  ion is coordinated by His<sup>45</sup>, Cys<sup>86</sup>, His<sup>91</sup>, and Gln<sup>96</sup> in a distorted tetrahedron, the distances of the Cu-His<sup>45</sup>, Cu-Cys<sup>86</sup>, Cu-His<sup>91</sup>, and Cu-Gln<sup>96</sup> ligands being 2.08, 2.17, 1.99, and 2.08 Å, respectively (Fig. 3). The parameters of the copper binding sites in CST, CBP, and two

crystal forms of a mutant azurin, M121Q (25), are summarized in Table 1. Comparison of the copper geometries revealed that oxidized mavicyanin has a shortened  $\text{Cu}^{\text{II}}$ - $\epsilon$ -O-Gln<sup>96</sup> distance, 2.08 Å, for coordinating the slight difference in the visible absorption spectrum at 448, 599, and 830 nm. The coordinating absorption bands of CST appear at 450, 604, and 850 nm, being slightly red-shifted compared to the above values for mavicyanin (8). In the copper binding site of reduced mavicyanin, the Cu-His<sup>45</sup>, Cu-Cys<sup>86</sup>, Cu-His<sup>91</sup>, and Cu-Gln<sup>96</sup> ligand atom dis-

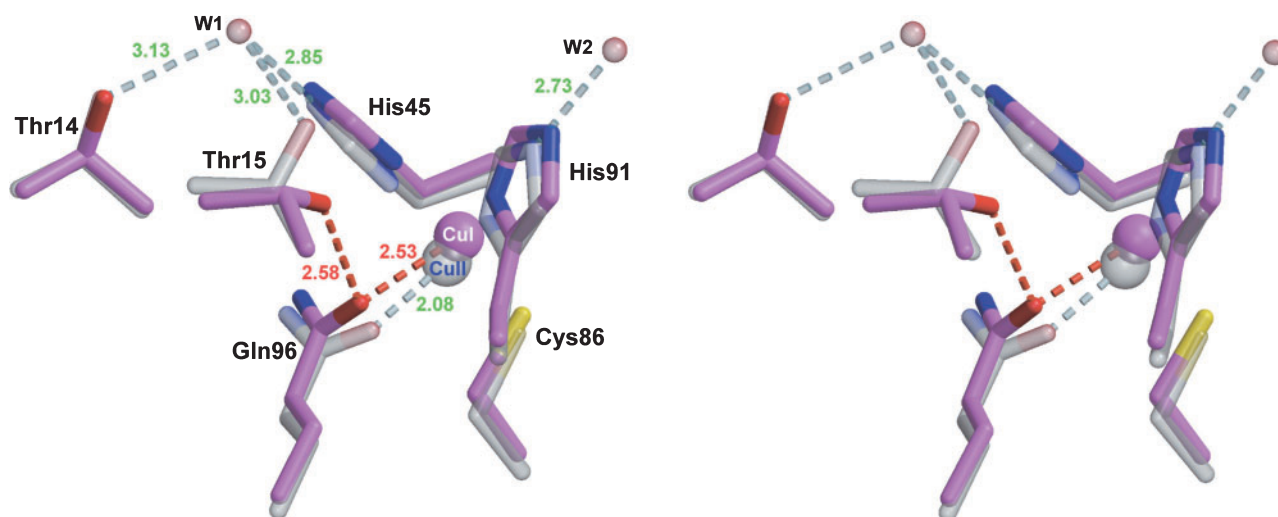


Fig. 5. Stereo view of structural comparisons around the copper binding structures between oxidized and reduced zucchini maviyanin. The  $\text{Cu}^{\text{II}}$  and  $\text{Cu}^{\text{I}}$  ions are shown as spheres, and the four ligands, His<sup>45</sup>, Cys<sup>86</sup>, His<sup>91</sup>, and Gln<sup>96</sup>, are represented by a stick model. The nitrogen, oxygen and sulfate atoms are shown in

tances are 2.12, 2.22, 2.07, and 2.53 Å, respectively (Fig. 4). The bond lengths of Cu-His<sup>45</sup>, Cu-Cys<sup>86</sup> and Cu-His<sup>91</sup> did not change upon reduction; however, the  $\text{Cu}^{\text{II}}-\epsilon\text{-O-Gln}^{\text{96}}$  bond length was extended by 0.47 Å.

In the oxidized form, each of the two His ligands is hydrogen bonded with a water molecule. The distance between  $\epsilon\text{-N-His}^{\text{45}}$  and the water molecule (W1) is 2.85 Å. W1 also hydrogen bonds with Thr<sup>14</sup> and Thr<sup>15</sup>. The W1- $\gamma\text{1O-Thr}^{\text{14}}$  and W1- $\gamma\text{1-O-Thr}^{\text{15}}$  distances are 3.13 Å and 3.03 Å, respectively. The distance between  $\epsilon\text{-N-His}^{\text{91}}$  and the water molecule (W2) is 2.73 Å. In the copper center of the reduced form, the two His ligands do not form hydrogen bonds with the solvent molecules. The axial ligand Gln<sup>96</sup> moves away from the copper ion to form a new hydrogen bond with  $\gamma\text{1-O-Thr}^{\text{15}}$ . The distance between  $\epsilon\text{O-Gln}^{\text{96}}$  and  $\gamma\text{1-O-Thr}^{\text{15}}$  in the oxidized form was calculated to be 4.78 Å; however, the distance decreased to 2.58 Å upon reduction, and a new hydrogen bond was formed between  $\epsilon\text{O-Gln}^{\text{96}}$  and  $\gamma\text{1-O-Thr}^{\text{15}}$  in this reduced form (Fig. 5). Superimposition of the oxidized and reduced forms reveals that the Thr<sup>15</sup> is dramatically rotated 60.0 by degrees. The hydrogen bond network involving W1, Thr<sup>14</sup>, Thr<sup>15</sup>, and His<sup>45</sup>, which was found in the oxidized form, was obviously broken on the rotation of Thr<sup>15</sup>, suggesting that the new hydrogen bond may stabilize the structure of the reduced copper binding site.

Battistuzzi and co-workers found that maviyanin shows an increased  $E^{\circ}$  below pH 4, due to protonation and detachment of a His ligand from  $\text{Cu}^{\text{I}}$  (15). The structure of reduced maviyanin shows that neither His ligand binds a solvent molecule, suggesting the His ligands are easily protonated at low pHs, which may constitute structural evidence for an increase in  $E^{\circ}$  below pH 4. On the other hand, maviyanin also showed decreases in  $E^{\circ}$  above pH 8, which were caused by the ionization of a residue that changes the copper coordination geometry, however, the residue was not identified (16). Thr<sup>15</sup> is easily ionized at high pH. The rotation of Thr<sup>15</sup> and the hydro-

gen bonding with the ligand Gln<sup>96</sup> may constitute structural evidence for a decreased reduction potential above pH 8.

The atomic coordinates and structure factors of the oxidized maviyanin and reduced maviyanin have been deposited in the Protein Data Bank, Research Collaboratory for Structural Bioinformatics, Rutgers University, New Brunswick, NJ, with codes of 1WS8 and 1WS7, respectively.

This study was supported by a Grant-in-Aid for Scientific Research from the Ministry of Education, Culture, Sports, Science and Technology of Japan, NEDO and the PRESTO project, Japan Science and Technology Corporation (to T. I.), the National Project on Protein Structural and Functional Analyses, Japan (to S. S.), and the center of excellence (21COE) program "Creation of Integrated EcoChemistry of Osaka University" (to Y. X.). The authors are grateful to Drs H. Kawamoto and K. Miura for the MAD data collection at the SPring-8 beam line.

## REFERENCES

- Adman, E.T. (1991) Copper protein structures. *Adv. Protein Chem.* **43**, 145–197
- Solomon, E.I., Baldwin, M.J., and Lowery, M.D. (1992) Electronic structures of active sites in copper proteins: Contribution to reactivity. *Chem. Rev.* **92**, 521–542
- Nersissian, A.M. and Shipp, E.L., (2002) Blue copper-binding domains. *Adv. Protein Chem.* **60**, 271–340
- Ryden, L.G. and Hunt, L.T. (1993) Evolution of protein complexity: the blue copper-containing oxidases and related proteins. *J. Mol. Evol.* **36**, 41–66
- Nersissian, A.M., Immoos, C., Hill, M.G., Hart, P.J., Williams, G., Herrmann, R.G., and Valentine, J.S. (1998) Uclacyanins, stellacyanins, and plantacyanins are distinct subfamilies of phytocyanins: plant-specific mononuclear blue copper proteins. *Protein Sci.* **7**, 1975–1929
- Marchesini, A., Minelli, M., Merkle, H., and Kroneck, P.M. (1979) Maviyanin, a blue copper protein from *Cucurbita pepo medullosa*. *Eur. J. Biochem.* **101**, 77–84

7. Schinina, M.E., Maritano, S., Barra, D., Mondovi, B., and Marchesini, A., (1996) Mavicyanin, a stellacyanin-like protein from zucchini peelings: a primary structure and comparison with other cupredoxins. *Biochim. Biophys. Acta* **1297**, 28–32
8. Maritano, S., Marchesini, A., and Suzuki, S., (1997) Spectroscopic characterization of native and Co(II)-substituted zucchini mavicyanin. *J. Biol. Inorg. Chem.* **2**, 177–181
9. Kataoka, K., Nakai, M., Yamaguchi, K., and Suzuki, S., (1998) Gene synthesis, expression, and mutagenesis of zucchini mavicyanin: the fourth ligand of blue copper center is Gln. *Biochem. Biophys. Res. Commun.* **250**, 409–413
10. Kataoka, K., Kondo, A., Yamaguchi, K., and Suzuki, S. (2000) Spectroscopic and electrochemical properties of the Met86Gln mutant of *Achromobacter cycloclastes* pseudoazurin. *J. Inorg. Biochem.* **82**, 79–84
11. Guss, J.M., Merritt, E.A., Phizackerley, R.P., and Freeman, H.C. (1996) The structure of a phytocyanin, the basic blue protein from cucumber, refined at 1.8 Å resolution. *J. Mol. Biol.* **262**, 686–705
12. Hart, P.J., Nersissian, A.M., Herrmann, R.G., Nalbandyan, R.M., Valentine, J.S., and Eisenberg, D. (1996) A missing link in cupredoxins: crystal structure of cucumber stellacyanin at 1.6 Å resolution. *Protein Sci.* **5**, 2175–2183
13. Battistuzzi, G., Borsari, M., Loschi, L., and Sola, M. (1997) Redox thermodynamics, acid-base equilibria and salt-induced effects for the cucumber basic protein. General implications for blue-copper proteins. *J. Biol. Inorg. Chem.* **2**, 350–359
14. Battistuzzi, G., Borsari, M., Loschi, L., and Sola, M. (1998) Redox properties of the basic blue protein (plantacyanin) from spinach. *J. Inorg. Biochem.* **69**, 97–100
15. Battistuzzi, G., Borsari, M., Loschi, L., Ranieri, A., Sola, M., Mondovì, B., and Marchesini, A., (2001) Redox properties and acid-base equilibria of zucchini mavicyanin. *J. Inorg. Biochem.* **83**, 223–227
16. Fernandez, C.O., Sannazzaro, A.I., and Vila, A.J. (1997) Alkaline transition of *Rhus vernicifera* stellacyanin, an unusual blue copper protein. *Biochemistry* **36**, 10566–10570
17. Xie, Y., Inoue, T., Miyamoto, Y., Matsumura, H., Kataoka, K., Yamaguchi, K., Suzuki, S., and Kai, Y. (2003) Crystallization and preliminary X-ray crystallographic studies of mavicyanin from *Cucurbita pepo medullosa*. *Acta Cryst.* **D59**, 1474–1476
18. Otwinowski, Z. and Minor, W. (1997) Processing of X-ray diffraction data collected in oscillation mode. *Methods Enzymol.* **276**, 307–326
19. Brunger, A.T., Adams, P.D., Clore, G.M., Delano, W.L., Gros, P., Grosse-Kunstleve, R.W., Jiang, J.-S., Kuszewski, J., Nilges, M., Pannu, N.S., Read, R.J., Rice, L.M., Simonson, T., and Warren, G.L. (1998) Crystallography & MNR system: a new software suite for macromolecular structure determination. *Acta Cryst.* **D54**, 905–921
20. Jones, T.A., Zou, J.-Y., Cowan, S.W., and Kjeldgaard, M. (1991) Improves methods for building protein models in electron density maps and location of errors in these models. *Acta Cryst.* **A47**, 110–119
21. Jones, T.A. (1985) Diffraction methods for biological macromolecules. Interactive computer graphics: FRODO. *Methods Enzymol.* **115**, 157–171
22. Navaza, J. (1994) *AMoRe*: an automated package for molecular replacement. *Acta Cryst.* **A50**, 157–163
23. Collaborative Computational Project, Number 4 (1994) The CCP4 suite: programs for protein crystallography. *Acta Cryst.* **D50**, 760–763
24. Laskowski, R.A. (1993) *PROCHECK*: a program to check the stereochemical quality of protein structures. *J. Appl. Crystallogr.* **26**, 283–291
25. Romero, A., Hoitink, C.W.G., Nar, H., Huber, R., Messerschmidt, A., and Canters, G.W., (1993) X-ray analysis and spectroscopic characterization of M121Q azurin: A copper site model for stellacyanin. *J. Mol. Biol.* **229**, 1007–1021
26. Kraulis, P.J. (1991) *MOLSCRIPT*: a program to produce both detailed and schematic plots of protein structures. *J. Appl. Crystallogr.* **24**, 946–950
27. Ferrin, T.E., Huang, C.C., Jarvis, L.E., and Langridge, R. (1988) The MIDAS display system. *J. Mol. Graphics* **6**, 13–27
28. Huang, C.C., Pettersen, E.F., Klein, T.E., Ferrin, T.E., and Langridge, R. (1991) Conic: A fast renderer for spacefilling molecules with shadows. *J. Mol. Graphics* **9**, 230–236
29. Barton, G.J. (1993) *ALSCRIPT*: a tool to format multiple sequence alignments. *Protein Eng.* **6**, 37–40